

An Adaptive Compliance Hierarchical Quadratic Programming Controller for Ergonomic Human-Robot Collaboration

Francesco Tassi^{a,b}, Elena De Momi^b, Arash Ajoudani^a

^aHRI² Lab of Italian Institute of Technology (IIT), Genoa, Italy

^bDepartment of Electronics, Information and Bioengineering, Politecnico di Milano, Milan, Italy

Abstract

This paper proposes a novel Augmented Hierarchical Quadratic Programming (AHQP) framework for multi-tasking control in Human-Robot Collaboration (HRC) which integrates human-related parameters to optimize ergonomics. The aim is to combine parameters that are typical of both industrial applications (e.g. cycle times, productivity) and human comfort (e.g. ergonomics, preference), to identify an optimal trade-off. The augmentation aspect avoids the dependency from a fixed end-effector reference trajectory, which becomes part of the optimization variables and can be used to define a feasible workspace region in which physical interaction can occur. We then demonstrate that the integration of the proposed AHQP in HRC permits the addition of human ergonomics and preference. To achieve this, we develop a human ergonomics function based on the mapping of an ergonomics score, compatible with AHQP formulation. This allows to identify at control level the optimal Cartesian pose that satisfies the active objectives and constraints, that are now linked to human ergonomics. In addition, we build an adaptive compliance framework that integrates both aspects of human preferences and intentions, which are finally tested in several collaborative experiments using the redundant MOCA robot. Overall, we achieve improved human ergonomics and health conditions, aiming at the potential reduction of work-related musculoskeletal disorders.

Keywords: Hierarchical control, adaptive compliance, human-robot collaboration, inverse kinematics, redundancy, human ergonomics

1. Introduction

While conducting an activity, a human is capable of taking into account more than one aspect that might affect the task at hand. In fact, there are multiple factors that we tend to naturally consider when planning and performing our actions, e.g., physical and spatial limitations and time constraints. As a consequence, for a robot to efficiently collaborate with a human, we must expect similar capabilities and behaviours, together with a good degree of flexibility with respect to unforeseen circumstances, typical of realistic collaborative scenarios.

Indeed, it is common to have a large number of limitations dictated by either external surroundings, target tasks or by robot mechanics. Thereby, to ensure task feasibility under multiple constraints it is important to define different priority levels that do not conflict with each other.

Early studies [1], set the basis for this concept by exploiting the redundancy of robot manipulators. Here the Jacobian matrix was used to obtain the general solution to the redundant kinematics problem, and a gradient vector of a scalar function was proposed in order to define an arbitrary secondary task. By projecting this in the null-space of the Jacobian matrix it was possible to avoid any interference with the primary task.

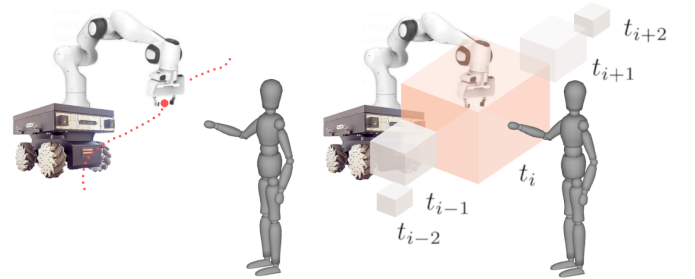


Figure 1: With a standard HQP controller (left), the fixed reference trajectory dictates the point of physical interaction. This ties the controller to motion planning stage, limiting autonomy and forcing the human to adapt to the robot. The proposed AHQP controller (right), defines a shared workspace (illustrated through the boxes, with the red one being active at current time t_i), whose size varies based on whether HRC should or should not occur. Inside this, the robot identifies the optimal pose based on the hierarchy of tasks. In HRC, this implies the robot adapting to the human and not vice versa.

From this, the redundant kinematics problem could be solved at different levels, namely velocity [2], acceleration [3, 4, 5] and force [6] levels.

The possibility of managing multiple objectives in the same task [5], led to all the following studies on hierarchical control techniques. Currently, the number of applications ranges from multiple robots [7, 8] to medical robots [9], teleoperation [10]

*Corresponding authors

Email address: francesco.tassi@iit.it (Francesco Tassi)

and humanoids control [11, 12]. In general, the methods for dealing with hierarchical control schemes can be classified into strict and non-strict hierarchies. A non-strict hierarchy [13, 14] is based on the attribution of a set of gains to each objective, and its advantages are related to simplicity and computational lightness. However, it is not possible to restrict a task having a lower priority in the null-space of the task that has a higher priority. Overall, this scheme is favoured when the number of objectives/constraints (and thus the degree of redundancy) is limited.

A strict hierarchy instead, is based on the definition of a stack of tasks, in which to every task is assigned a priority level, that is enforced by projecting the secondary task into the null-space of the primary one. One of the most common techniques is Hierarchical Quadratic Programming (HQP) [15, 16]. This attributes to each element of the stack a Quadratic Programming (QP) problem, that is solved hierarchically under equality/inequality constraints [17, 18]. The Inverse Kinematics (IK) of the robot is formulated as a QP problem, allowing to identify the optimal joint trajectories of the redundant robot.

Classic HQP-based IK formulations however, require as input the specific reference trajectories that should be followed by the End-Effector (EE). This is clearly necessary for most controllers, but it lowers the autonomy and adaptability to unstructured environments. Besides, it is easy to think to a great variety of applications in which this is not beneficial. In Human-Robot Collaboration (HRC) for example, ideally the robot is able to identify and vary autonomously the optimal trajectory to follow, without relying on preset trajectories that are tied to the specific task.

To address this issue, we recently proposed an Augmented HQP (AHQP) control scheme for the solution of the IK problem [19], in which the Cartesian reference is now part of the optimization variables. This allowed to reduce the controller's dependency from a fixed trajectory predefined at upper level, requiring as input only constraints and objectives definition. This is in line with the important concept of functional autonomy often raised by the authors of [20], for which a controller should require a smaller set of control inputs necessary for controlling a (possibly highly) redundant robot, to increase its flexibility of application to unstructured environments. Therefore, detaching from the conventional idea of planning and then executing, which inherently creates a real-time gap, allows instead to aim for increased synergy between planning and control.

This paper constitutes an evolved version of our past work according, with the following novel contributions. Firstly, we integrate human factors in the AHQP problem thanks to a human ergonomics mapping, with the aim of optimizing posture, and reducing MusculoSkeletal Disorders (MSDs), which have been directly linked to considerable economic losses in the industrial environment [21]. In addition, we develop and integrate the aspect of human preference through the definition of an adaptive compliance framework that is based on the augmented structure. This allows to accommodate for the individual preference of the worker while still accounting for optimal ergonomics.

In the end, the controller will be capable of optimizing not

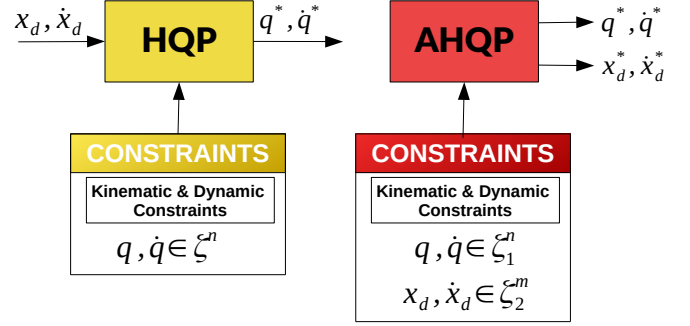


Figure 2: Block diagrams comparing the hierarchical solution of the IK problem. Classical HQP control scheme (left), and Augmented HQP [19] (right).

only the efficiency of the task (e.g., cycle times reduction, increased productivity) but also human-related parameters simultaneously (e.g., ergonomics, preference).

1.1. Contributions

A detailed survey on the latest advancements of HRC in the manufacturing industry [22] also shows the relevance of industrial HRC, not only limited to the use of collaborative robots. Multiple open challenges are listed, which are mainly related to the lack of lightweight methods for the evaluation of HRC task performance as well as human quantities in task planning. With the present work, we face both issues, not only by optimally planning directly at control level, but also by integrating human ergonomics online for rapid robot's adaptation.

The reasons why the augmented scheme is essential to create a flexible planning and execution in HRC tasks are the following:

- to exploit the aforementioned advantages of higher flexibility in unpredicted contexts
- to map offline the human ergonomics, avoiding cumbersome human kinematics models running online (as it is often done in the literature [22, 23]) and not having to rely on noisy acquisitions of all human joints coordinates, since only human's location is required online
- to integrate human ergonomics as a compatible objective function that can be optimized in the stack of tasks online
- to provide an adaptive compliance control framework useful to accommodate human preferences in the same hierarchy.

In Fig. 1 we provide a graphical comparison for the use of AHQP in HRC. On the left, a standard HQP-based controller receives as input a precise reference trajectory, that is followed strictly by the robot, to which the human has to adapt for engaging in the HRC. On the right, the AHQP allows to define a feasible area for each time t_i , shown in red, that is defined at constraints level. This acts as a shared workspace, inside of which the optimization will identify the optimal point for physical interaction. Therefore, based on the active objective

functions defined in the stack of tasks, this will result in the robot adapting to human needs and not vice versa. Overall, this work's contributions can be listed as follows.

- A Cartesian space mapping of human ergonomics is generated, which establishes the relation between posture and ergonomics score.
- Optimal human ergonomics is formulated in the stack of tasks of a hierarchical controller in QP form, through the mapping defined.
- An AHQP-based adaptive compliance framework is constructed, based on the varying EE's trajectory as the augmented variable. This allows to respond adaptively, based on the type of forces exchanged (i.e. human or environment).
- The adaptive compliance framework is extended to integrate human preference in the task. We finally achieve an ergonomics-aware AHQP framework that includes human preference along with secondary robot-related objectives.

The proposed control structure is validated through several experiments, conducted using the MOBILE Collaborative robotic Assistant (MOCA). Overall, we note a remarkable increase in both the ergonomics and the efficiency of HRC.

To summarize, the plan of the paper is as follows. We start in Sec. 2 by recalling the classical HQP formulation, together with its augmented version of the AHQP. In Sec. 3 we describe the proposed controller, which we then used to conduct the experiments of Sec. 4. Finally, in Sec. 5 we give a brief discussion on the obtained results and draw some conclusions, framing our work in a broader context for future developments.

2. Methods

In this section we firstly review the basic formulation of the HQP scheme commonly used for IK resolution, and we then report the AHQP formulation that will be used for the proposed framework in Sec. 3.

2.1. Hierarchical Quadratic Programming

Using a redundant robot it is possible to define a sequence of secondary objectives that need to be accomplished without altering the performances of the primary one, leading to the generation of a hierarchical stack of tasks that exploits the whole-body motion of the robot [24]. Indeed, by considering $k \in \{1, \dots, p\}$ levels of priority where the importance decreases with k down to the last task p , we ensure that the solutions found at level k are always strictly enforced at the lower priority level $k+1$, which constitutes the main reason behind the choice of a strict priority scheme [17].

The k^{th} generic and robot-independent hierarchical problem can thus be written as:

$$\begin{aligned} \min_{\chi} \quad & \frac{1}{2} \|A_k \chi - b_k\|^2 \\ \text{s.t.} \quad & C_1 \chi \leq d_1 \\ & \vdots \\ & C_k \chi \leq d_k \\ & E_1 \chi = f_1 \\ & \vdots \\ & E_k \chi = f_k \end{aligned} \quad (1)$$

$\chi \in \mathbb{R}^s$ being the generic variable to optimize, n_k is the dimension of the k -th task, subject to n_{e_k} and n_{i_k} dimensional equality and inequality constraints respectively, through matrices $A_k \in \mathbb{R}^{n_k \times s}$, $C_k \in \mathbb{R}^{n_{i_k} \times s}$, $E_k \in \mathbb{R}^{n_{e_k} \times s}$ and vectors $b_k \in \mathbb{R}^{n_k}$, $d_k \in \mathbb{R}^{n_{i_k}}$, $f_k \in \mathbb{R}^{n_{e_k}}$.

The previous $1, \dots, k-1$ solutions are addressed through the optimality condition between successive tasks $A_{k-1} \chi = A_{k-1} \chi_{k-1}^*$ whose demonstration is reported in [17]. In this way, the optimality of the tasks with higher priority is not altered by the actual solution, and it can be added in (1) as a set of equality constraints by considering $E_1 = \mathbf{0}$, $f_1 = \mathbf{0}$, up to $E_k = A_{k-1}$, $f_k = A_{k-1} \chi_{k-1}^*$.

We consider now an n degrees of freedom redundant robot, with desired joint velocity $\dot{\mathbf{q}} \in \mathbb{R}^n$, and task space velocity $\dot{\mathbf{x}} \in \mathbb{R}^m$. The IK problem in QP form is:

$$\min_{\dot{\mathbf{q}}} \|\mathbf{J} \dot{\mathbf{q}} - \dot{\mathbf{x}}\|^2 \quad (2)$$

where $\mathbf{J}(\mathbf{q}) \in \mathbb{R}^{m \times n}$ is the task Jacobian matrix. In addition, a Closed-Loop IK (CLIK) scheme is used to recover from position errors between the desired and actual behaviour

$$\min_{\dot{\mathbf{q}}} \|\mathbf{J} \dot{\mathbf{q}} - (\dot{\mathbf{x}}_d + \mathbf{K}_p(\mathbf{x}_d - \mathbf{x}_a))\|^2, \quad (3)$$

where $\mathbf{x}_a, \mathbf{x}_d \in \mathbb{R}^m$ are the actual and desired Cartesian poses of the EE respectively and $\mathbf{K}_p \in \mathbb{R}^{m \times m}$ is the positive-definite diagonal gain matrix responsible for error convergence.

2.2. Augmented HQP

Often in real applications, instead of a fixed initial and final target pose, it is beneficial to define a final feasible region, while at the same time e.g. accounting for obstacle avoidance, singularity avoidance or even human ergonomics. This is the purpose of the AHQP scheme shown in Fig. 2 (right). As opposed to the classical formulation (left), here the desired EE trajectories are not provided as inputs, being instead part of the outcome by augmenting the state variable $\chi \in \mathbb{R}^{s=n+m}$:

$$\chi = \begin{bmatrix} \dot{\mathbf{q}} \\ \dot{\mathbf{x}}_d \end{bmatrix} \quad (4)$$

In this case, the only inputs are the constraints, which can now be defined as well directly with respect to Cartesian coordinates. A feasibility region for $\dot{\mathbf{x}}_d, \mathbf{x}_d$ is then defined, in which

the optimal output pose will lie. The optimal \mathbf{q}^* , $\dot{\mathbf{q}}^*$ that will be obtained from (1) are passed to the lower level joint impedance controller, which generates the necessary actuation torques

$$\boldsymbol{\tau} = \mathbf{K}_{q_d}(\dot{\mathbf{q}}^* - \dot{\mathbf{q}}_a) + \mathbf{K}_{q_p}(\mathbf{q}^* - \mathbf{q}_a) + \mathbf{g}(\mathbf{q}_a) \quad (5)$$

where $\dot{\mathbf{q}}_a, \mathbf{q}_a \in \mathbb{R}^n$ are the actual joint velocities and positions respectively, $\mathbf{K}_{q_p}, \mathbf{K}_{q_d} \in \mathbb{R}^{n \times n}$ are the positive definite joint stiffness and damping matrices respectively, while $\mathbf{g}(\mathbf{q}) \in \mathbb{R}^n$ is the gravity compensation term. Writing (3) in augmented form

$$\begin{aligned} \min_{\dot{\mathbf{q}}, \mathbf{x}_d} & \left\| \begin{bmatrix} \mathbf{J} & -(\mathbf{I} + \mathbf{K}_p \Delta t) \end{bmatrix} \begin{bmatrix} \dot{\mathbf{q}} \\ \mathbf{x}_d \end{bmatrix} - \mathbf{K}_p(\mathbf{x}_d(t - \Delta t) - \mathbf{x}_a) \right\|^2 \\ & = \min_{\chi \in \Omega} \|\mathbf{A}_1 \chi - \mathbf{b}_1\|^2 \end{aligned} \quad (6)$$

we can refer to the structure of (1), where $\Omega \subset \mathbb{R}^{s=n+m}$ is a non-empty convex set, Δt is the control period and $\mathbf{x}_d(t - \Delta t)$ is the value of \mathbf{x}_d at the previous time instant.

2.3. Constraints

As already mentioned, constraints definition is essential for the AHQP to specify a behaviour that the robot should abide by. Indeed, it is now possible to identify an additional set of task space constraints that characterize the shared workspace visible in Fig. 1. These are defined together with the classic joint space constraints that account for actuators range of motion, velocity and acceleration limits as:

$$\begin{aligned} \mathbf{q}_{min} & \leq \mathbf{q}(t - \Delta t) + \dot{\mathbf{q}}(t)\Delta t \leq \mathbf{q}_{max} \\ \dot{\mathbf{q}}_{min} & \leq \dot{\mathbf{q}} \leq \dot{\mathbf{q}}_{max} \\ \ddot{\mathbf{q}}_{min} & \leq \frac{\dot{\mathbf{q}}(t) - \dot{\mathbf{q}}(t - \Delta t)}{\Delta t} \leq \ddot{\mathbf{q}}_{max} \end{aligned} \quad (7)$$

to which we add

$$\begin{aligned} \mathbf{x}_{d_{min}} & \leq \mathbf{x}_d(t - \Delta t) + \dot{\mathbf{x}}_d(t)\Delta t \leq \mathbf{x}_{d_{max}} \\ \dot{\mathbf{x}}_{d_{min}} & \leq \dot{\mathbf{x}}_d \leq \dot{\mathbf{x}}_{d_{max}} \\ \ddot{\mathbf{x}}_{d_{min}} & \leq \frac{\dot{\mathbf{x}}_d(t) - \dot{\mathbf{x}}_d(t - \Delta t)}{\Delta t} \leq \ddot{\mathbf{x}}_{d_{max}} \end{aligned} \quad (8)$$

which describe position, velocity and acceleration limits respectively. It is then possible to express these constraints as a function of χ in augmented form as:

$$\frac{1}{\Delta t} \begin{pmatrix} \mathbf{q}_{min} - \mathbf{q}(t - \Delta t) \\ \mathbf{x}_{d_{min}} - \mathbf{x}_d(t - \Delta t) \end{pmatrix} \leq \chi \leq \frac{1}{\Delta t} \begin{pmatrix} \mathbf{q}_{max} - \mathbf{q}(t - \Delta t) \\ \mathbf{x}_{d_{max}} - \mathbf{x}_d(t - \Delta t) \end{pmatrix} \quad (9)$$

$$\chi_{min} \leq \chi \leq \chi_{max} \quad (10)$$

$$\begin{pmatrix} \dot{\mathbf{q}}(t - \Delta t) + \ddot{\mathbf{q}}_{min}\Delta t \\ \dot{\mathbf{x}}_d(t - \Delta t) + \ddot{\mathbf{x}}_{d_{min}}\Delta t \end{pmatrix} \leq \chi \leq \begin{pmatrix} \dot{\mathbf{q}}(t - \Delta t) + \ddot{\mathbf{q}}_{max}\Delta t \\ \dot{\mathbf{x}}_d(t - \Delta t) + \ddot{\mathbf{x}}_{d_{max}}\Delta t \end{pmatrix} \quad (11)$$

which binds the augmented state variable. Through this, we are essentially setting the boundaries for physical interaction (Fig. 1 on the right, shows these boundaries at position level, active at different times during the task, which reflect the shared workspace), allowing to obtain the EE trajectory online, based on the objectives defined in the stack of tasks and their relative priority.

3. Ergonomics-Aware AHQP

In this section, we introduce human ergonomics in the AHQP control scheme, with the aim of improving the quality of human-robot interaction. This will optimize in real-time the robot trajectory, based on the actions performed by the human. The aim is to first identify a suitable ergonomics score, capable of reflecting the health risks related to the human posture. Subsequently, by formulating the score as a function of the Cartesian coordinate, it will be possible to include the ergonomics in the hierarchical stack of tasks of the AHQP scheme. Finally, we include the aspect of human preference when performing a task, and its effects on ergonomics that are not considered by the scores. This is used to find a trade-off between optimal ergonomics and preference, exploiting the adaptive hierarchy of the AHQP.

3.1. Human Ergonomics Cartesian Mapping

The study on ergonomics is useful to minimize the adverse effects of incorrect habits and postures on workers, who are daily exposed to MSDs due to long-term fatigue accumulation and repetitive loading cycles. To avoid this, a key aspect is to maintain a good balance between the efforts and the ability to recover from fatigue [25]. The lack of this balance increases the probability of the workers to develop MSDs. For this reason, the aid of a collaborative robot (cobot) can prove fundamental not only when dealing with heavy objects, but also in other apparently simple but repetitive tasks. A large number of studies, in the literature [26, 27], use ergonomic assessment tools such as Rapid Upper Limb Assessment (RULA) and Rapid Entire Body Assessment (REBA) scores [28]. These scores are expressed as a function of the human joint angles configuration as follows and a higher score corresponds to a more critical position:

$$E_s = h(\mathbf{q}_h), \quad (12)$$

where $E_s \in \mathbb{Z}$ is the integer ergonomics score that corresponds to the human posture \mathbf{q}_h when reaching the pose $\mathbf{x}_h \in \mathbb{R}^m$ with the human's dominant hand.

Given the highly discrete nature of the final REBA score, we instead consider its intermediate scores, which describe separately the contributions of the arms, trunk, legs and neck. We average these contributions with different weights, to achieve a more sensitive variation to different postures, which is useful to lessen the score's discrete nature.

Being interested in the collaboration between human and robot, we will consider $\mathbf{x}_h = \mathbf{x}_d$ throughout the remainder of the work, since we are considering the period in which the physical interaction occurs. This will allow us to account for human ergonomics in the AHQP scheme, by formulating it in function of \mathbf{x}_d which is now part of the optimization variable. Therefore, the human posture is considered only offline (through the mapping), not having to extend the state with \mathbf{q}_h , and not requiring complex human kinematics modelling [23], which would result in over-demanding computations for real-time purposes. Hence, the score is mapped in the human-robot shared workspace

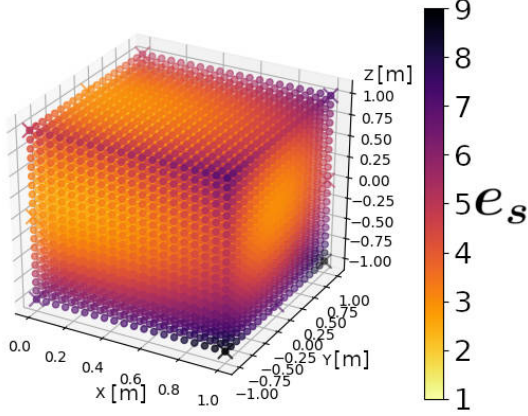


Figure 3: Cartesian mapping of the REBA ergonomics score e_s for human's hand position \mathbf{x}_h in human frame (human's center of mass in standing conditions, facing towards positive x -axis), obtained interpolating the scores achieved in a total of 150 points per subject. A higher score (darker color) indicates a less ergonomic posture (1 being a safe posture, while 9+ highly risky).

defined thanks to (8), to achieve a continuous ergonomics function compatible in QP form as

$$e_s = l(\mathbf{x}_d), \quad (13)$$

with the ergonomics score $e_s \in \mathbb{R}$ now as a function of the Cartesian coordinate \mathbf{x}_d , to be implemented in the AHQP.

For the mapping, we can acquire multiple human body postures for different Cartesian points, while performing a task. Accordingly, a set of postures is obtained for each position of the active human hand \mathbf{x}_h , and the corresponding scores E_s are calculated using the assessment criteria, based on the whole human joints configuration. In particular, each of the five subjects (four male and one female healthy subjects, all with similar height) was asked to reach 30 different points in the workspace for 5 times (for a total of 150 points per subject). As it was expected, by comparing among the entire human body postures, it was possible to notice both very similar hand's orientations and also human joint configurations, when reaching for the same point. This was obvious when comparing with the same subject, but it was also evident for the same point across all subjects.

For this reason, it was possible to consider, for each point, an average score normalized across all subjects, allowing to account for the small differences in posture (and thus in the REBA score), giving higher weight to more dangerous conditions (higher REBA score), to maintain an appropriate safety margin. Similarly, we attribute to each point the average rotation obtained from the measurements as the reference value. Finally, the Cartesian map can be generated through interpolation between the calculated ergonomics scores and the corresponding hand's coordinate (position + orientation), by formulating the interpolating function in QP form, as it will be discussed in Sec. 3.2. Fig. 3 shows the map obtained with a discretization step size of 20mm, where the origin corresponds to the coordinate of the human's centre of mass, while he/she is standing, and facing towards the positive x -axis. Fig. 4 helps to iden-

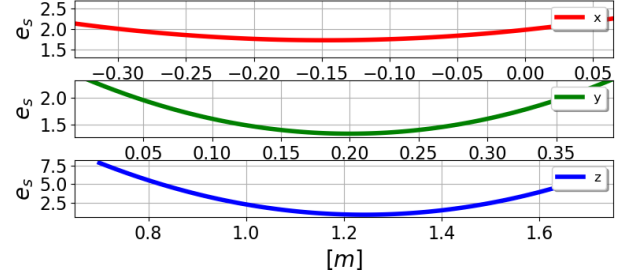


Figure 4: Convex ergonomics function e_s in world frame along directions x, y, z for a right-handed person standing on the origin $\mathbf{x}_h^w = (0, 0, 0)[m]$. The resulting global minimum is $\mathbf{x}_m^w = (-0.15, 0.2, 1.24)[m]$. The individual contributions are obtained by fixing the other two components at their global minimum.

tify the overall minimum point of the Cartesian map along each direction, keeping the other two fixed at their global minimum.

3.2. Human Ergonomics for HQP

We show in this section the addition of human ergonomics in the AHQP framework. Having to comply with QP form, we choose a quadratic interpolating function in which it is possible to include the parameters obtained from the interpolation

$$\begin{aligned} e_s = l(\mathbf{x}_d) &= \frac{1}{2} \mathbf{x}_d^T \begin{bmatrix} a_1 & & \\ & \ddots & \\ & & a_m \end{bmatrix} \mathbf{x}_d + \begin{bmatrix} b_1 \\ \vdots \\ b_m \end{bmatrix}^T \mathbf{x}_d \\ &= \frac{1}{2} \mathbf{x}_d^T \mathbf{H} \mathbf{x}_d + \mathbf{g}^T \mathbf{x}_d, \end{aligned} \quad (14)$$

where $\mathbf{H} \in \mathbb{R}^{m \times m}$ and $\mathbf{g} \in \mathbb{R}^m$ are the parameters matrix and vector respectively, whose parameters $a_1, \dots, a_m, b_1, \dots, b_m \in \mathbb{R}$ are obtained from the ergonomics mapping identified offline as in Sec. 3.1, corresponding to the quadratic function

$$e_s = \frac{1}{2} (a_1 x_{d_1}^2 + \dots + a_m x_{d_m}^2) + b_1 x_{d_1} + \dots + b_m x_{d_m}. \quad (15)$$

For our purpose, despite the highly nonlinear nature of the human kinematics, a quadratic representation of e_s (necessary to comply with the QP form) is adequate for correcting the human posture and promoting healthier positions. In addition, as from Fig. 3, this approximation also provides a higher safety margin.

Rewriting then (14) as a function of the Cartesian velocities $\dot{\mathbf{x}}_d$ for the AHQP scheme leads to

$$\begin{aligned} e_s = f(\dot{\mathbf{x}}_d) &= \frac{1}{2} (\mathbf{x}_{d_{t-1}} + \Delta t \dot{\mathbf{x}}_d)^T \mathbf{H} (\mathbf{x}_{d_{t-1}} + \Delta t \dot{\mathbf{x}}_d) \\ &+ \mathbf{g}^T (\mathbf{x}_{d_{t-1}} + \Delta t \dot{\mathbf{x}}_d) \end{aligned} \quad (16)$$

$$= \frac{1}{2} \Delta t^2 \dot{\mathbf{x}}_d^T \mathbf{H} \dot{\mathbf{x}}_d + \Delta t (\mathbf{x}_{d_{t-1}}^T \mathbf{H} + \mathbf{g}^T) \dot{\mathbf{x}}_d \quad (17)$$

$$= \frac{1}{2} \dot{\mathbf{x}}_d^T \mathbf{H}_n \dot{\mathbf{x}}_d + \mathbf{g}_n^T \dot{\mathbf{x}}_d \quad (18)$$

where Δt is the control period and $\mathbf{x}_{d_{t-1}} = \mathbf{x}_d(t - \Delta t)$. Finally,

the ergonomics function in augmented form becomes

$$\min_{\dot{q}, \dot{x}_d} e_s = \min_{\dot{q}, \dot{x}_d} f(\dot{x}_d) = \min_{\chi} f_a(\chi) \quad (19)$$

$$= \min_{\chi} \frac{1}{2} \chi^T \begin{bmatrix} \mathbf{0} & \mathbf{0} \\ \mathbf{0} & \mathbf{H}_n \end{bmatrix} \chi + \begin{bmatrix} \mathbf{0} \\ \mathbf{g}_n \end{bmatrix}^T \chi \quad (20)$$

$$= \min_{\chi} \frac{1}{2} \chi^T \mathbf{H}_{ergo} \chi + \mathbf{g}_{ergo}^T \chi \quad (21)$$

where $\mathbf{H}_{ergo} \in \mathbb{R}^{s \times s}$ and $\mathbf{g}_{ergo} \in \mathbb{R}^s$, and it can be minimized using the AHQP as in Algorithm 1. This will regulate the position in which the robot's EE and the human hand meet to perform the task, by optimizing human posture, as it will be demonstrated in the experiments.

3.3. Additional Robot-Related Tasks

We hereby formulate the additional objective functions in augmented form, useful for the implementation in the stack of tasks of our controller. The first one is the robot's *postural task*, which allows to impose a behaviour at joint level along its kinematic chain (e.g. minimum joint displacement from actuators mid-range). This is achieved by minimizing

$$\min_{\chi} \|\mathbf{q} - \mathbf{q}_{pos}\|^2, \quad (22)$$

with $\mathbf{q}_{pos} \in \mathbb{R}^n$ being the desired target joint positions. Rewriting in augmented form we obtain

$$\begin{aligned} \min_{\chi} \|\mathbf{q}(t - \Delta t) + \dot{\mathbf{q}}\Delta t - \mathbf{q}_{pos}\|^2 &= \\ \min_{\chi} \left\| \begin{bmatrix} \Delta t \mathbf{I}_{n \times n} & \mathbf{0}_{n \times m} \end{bmatrix} \begin{bmatrix} \dot{\mathbf{q}} \\ \dot{\mathbf{x}}_d \end{bmatrix} - (\mathbf{q}_{pos} - \mathbf{q}(t - \Delta t)) \right\|^2 &= \\ \min_{\chi} \|\mathbf{A}_{pos}\chi - \mathbf{b}_{pos}\|^2 & \end{aligned} \quad (23)$$

where $\mathbf{A}_{pos} \in \mathbb{R}^{n \times s}$ and $\mathbf{b}_{pos} \in \mathbb{R}^n$ allow to define the *postural task* inside of the hierarchy, as expressed in Algorithm 1. In addition, a regularization term is added through

$$\min_{\chi} \|\dot{\mathbf{q}}\|^2, \quad (24)$$

to ensure numerical stability [29, 30] and avoid sudden behaviours in the solution while switching between tasks.

Another task is the one related to Cartesian reference regulation, useful when it is necessary to reach a specific goal pose with the EE, which drives the desired \mathbf{x}_d to a target pose $\mathbf{x}_t \in \mathbb{R}^m$ through

$$\min_{\chi} \|\mathbf{x}_d - \mathbf{x}_t\|^2, \quad (25)$$

while also ensuring that the target pose lies inside the feasible region defined by the constraints on \mathbf{x}_d (8). Similarly to (23), we write (25) in augmented form as

$$\begin{aligned} \min_{\chi} \|\mathbf{x}_d(t - \Delta t) + \dot{\mathbf{x}}_d \Delta t - \mathbf{x}_t\|^2 &= \\ \min_{\chi} \left\| \begin{bmatrix} \mathbf{0}_{m \times n} & \mathbf{I}_{m \times m} \end{bmatrix} \begin{bmatrix} \dot{\mathbf{q}} \\ \dot{\mathbf{x}}_d \end{bmatrix} - (\mathbf{x}_t - \mathbf{x}_d(t - \Delta t)) \right\|^2 &= \\ \min_{\chi} \|\mathbf{A}_{cart}\chi - \mathbf{b}_{cart}\|^2 & \end{aligned} \quad (26)$$

with $\mathbf{A}_{cart} \in \mathbb{R}^{m \times s}$ and $\mathbf{b}_{cart} \in \mathbb{R}^m$. This is useful when the robot is not collaborating with the human, for which $\mathbf{x}_h = \mathbf{x}_d$ no longer holds, and thus the optimal ergonomics task is inactive. Indeed, it acts as some kind of planning for \mathbf{x}_d , which consequently affects \mathbf{x}_a through the CLIK in (6). An example will be provided in Sec 4.2 during the first experiment.

Similarly, it is possible to account for obstacle avoidance through various formulations of the objective functions [31], which, for the sake of clarity, we will not consider as part of the present work.

Algorithm 1: Adaptive compliance AHQP

Result: χ

Initial set of inequality constraints: $\mathbf{C}_1, \mathbf{d}_1$;

Initial set of equality constraints: $\mathbf{E}_1, \mathbf{f}_1$;

while $t > 0$ **do**

Data: $\mathbf{q}_a, \dot{\mathbf{q}}_a, \mathbf{x}_a, \dot{\mathbf{x}}_a$

 Stack of tasks definition/update:

if $\|\mathbf{e}_q\|_{\infty} = \|\mathbf{q} - \mathbf{q}_a\|_{\infty} \leq \text{threshold}$ **then**

$p = 4$;

$\mathbf{A}_1, \mathbf{b}_1 \leftarrow \text{CLIK (6)}$;

$\mathbf{A}_2, \mathbf{b}_2 \leftarrow \mathbf{H}_{ergo}, \mathbf{g}_{ergo}$ Ergonomics (21)

$\mathbf{A}_3, \mathbf{b}_3 \leftarrow \mathbf{A}_{pos}, \mathbf{b}_{pos}$ Postural task (23);

$\mathbf{A}_4, \mathbf{b}_4 \leftarrow \text{Regularization term (24)}$;

else

$p = 2$;

$\mathbf{A}_1, \mathbf{b}_1 \leftarrow \text{CLIK (6)}$;

$\mathbf{A}_2, \mathbf{b}_2 \leftarrow \text{Regularization term (24)}$;

 Update inequality/equality sets with online data;

 HQP:

for $k = 1$ **to** p **do**

 Solve the QP problem (1);

$\mathbf{C}_{k+1} \leftarrow \begin{bmatrix} \mathbf{C}_k \\ \mathbf{C}_{k+1} \end{bmatrix}, \mathbf{d}_{k+1} \leftarrow \begin{bmatrix} \mathbf{d}_k \\ \mathbf{d}_{k+1} \end{bmatrix}$;

$\mathbf{E}_{k+1} \leftarrow \begin{bmatrix} \mathbf{E}_k \\ \mathbf{A}_k \end{bmatrix}, \mathbf{f}_{k+1} \leftarrow \begin{bmatrix} \mathbf{f}_k \\ \mathbf{A}_k \chi_k^* \end{bmatrix}$;

3.4. Adaptive Compliance Framework

Typically in the literature, the forces exchanged during the physical interaction between human and robot are regulated by an adaptive controller, which feeds the torques and commands to the robot. Therefore, based on the type of interaction or on the task at hand, either an impedance or an admittance controller is used. To improve the interaction's quality, we aim at a control framework that can achieve the advantages of both scenarios, by complying to human actions while also rejecting external disturbances. Indeed, different studies show the unsatisfactory performances of impedance and admittance control when there are large changes in the environmental stiffness [32]. This limitation is due to their inherent nature. The performances of an ideal controller should prove satisfactory regardless of the environment.

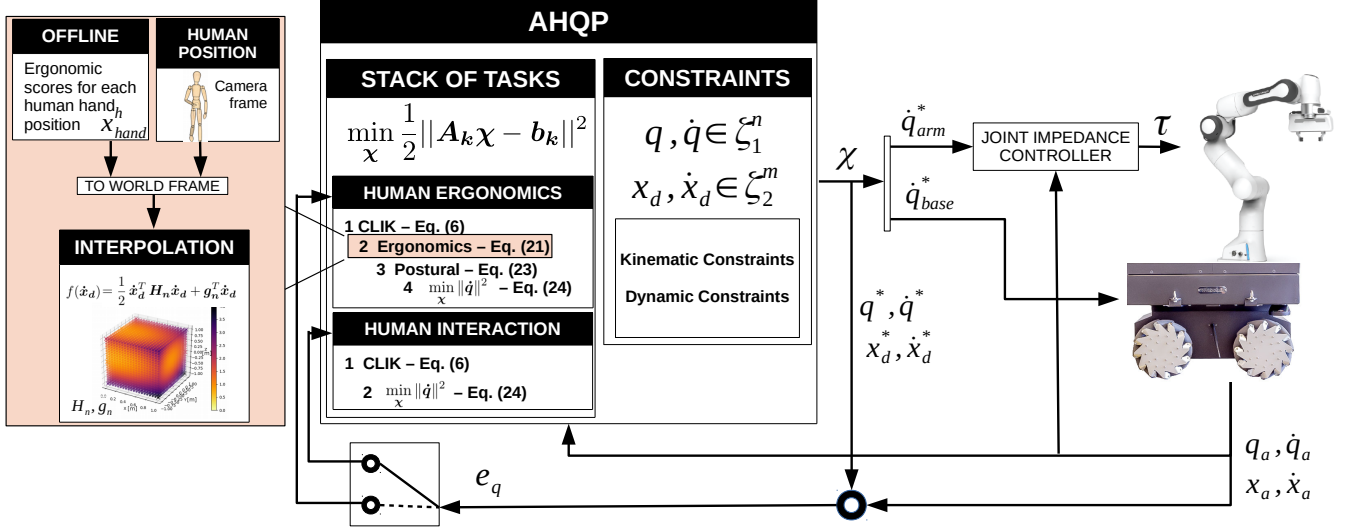


Figure 5: Block diagram of the proposed AHQP control framework for adaptive compliance with the inclusion of human ergonomics in the hierarchy. The parameters H_{ergo} and g_{ergo} obtained from the interpolation are fed to the stack of tasks definition of the HQP. Two modes (*human ergonomics* and *human interaction*) alternate based on joints position error $e_q = q_a - q^*$, allowing to switch between optimal ergonomics and force adaptation (useful for physical interaction, when the free variation of \dot{x}_d is allowed).

This motivates our choice of a mixed control strategy, which aims at the best of both cases. By exploiting the AHQP formulation we avoid having to generate a switching criteria between impedance and admittance mode, thus avoiding the problems related to discontinuities [32] during the switching phase, being the continuity of the solution enforced at constraints level. This provides safer physical interaction, accommodating the forces coming from the human and rejecting external perturbations.

For this reason, we exploit the AHQP framework as outlined in Fig. 5 and explained in Algorithm 1, acting on the robot behaviour by dynamically modifying the stack of tasks, based on the type of forces exchanged with the robot. Exploiting the possibility of varying \dot{x}_d in (4) we achieve the adaptive compliance behaviour by alternating the hierarchy as shown in Fig. 5 between *human ergonomics* and *human interaction* stacks. More practically, the Cartesian tasks regulating the desired EE pose x_d (in this case the optimal ergonomics map (21)) are removed from the hierarchy, and the only term responsible for x_d remains the CLIK (6) which will minimize the error with respect to the actual EE pose x_a . The collaboration with the human will lead to the displacement of the EE from its equilibrium pose, resulting in a progressive increase in the joint position error $e_q = q_a - q^*$, where q_a is the actual joints' position. This becomes the threshold for our dynamically alternating hierarchy between the two stack of tasks of Fig. 5 (Algorithm 1), to adapt in real-time the compliance level with respect to the physical interaction, without having to adjust the stiffness for the specific case.

Indeed, stiffness and gains regulation is often a limiting problem in robotic applications, which limits the robot adaptability to the specific scenario for which it is tailored. The gains used in the present framework will instead regulate how fast the robot will comply with respect to human intentions, but

the stiffness level will vary throughout the interaction. Finally, when the force exchange is over, the original hierarchy is restored (Fig. 5) and the new equilibrium conditions that result after the interaction are considered.

A common limitation when switching or modifying tasks with a hierarchical controller is related to discontinuities or jumps arising from the transition phase. Multiple works involve smooth transitioning between tasks for hierarchical control [33, 34]. In [35] the authors propose a simple strategy for the solution of robot's kinematics by defining a transitioning phase. In [36] a similar and more computationally efficient approach is proposed, which considers robot's dynamics and is based on constraints definition. Both methods can be implemented with the proposed AHQP structure without limitations, by accounting for the augmented state variable during the transition.

3.5. Human Preference Via Adaptive Compliance Framework

There are however some parameters, that are not properly detected by an ergonomic assessment technique like RULA and REBA, but that are somehow still related to the overall human ergonomics. As an example, by considering two physically similar subjects at kinematics level (height, arms/legs length, etc.), if we hand them a generic object in the same relative point, it is still possible that their grabbing method and arms/torso configuration will be different. This might be dictated for example by the amount of available muscle force, by the visual memory of a previous task, or more simply by the subject being right or left-handed. Since often the position in which human ergonomics is optimized does not correspond to the position the operator would spontaneously assume, a good compromise should be found between optimal ergonomics and human preference. Indeed, the preferences of the operator might affect the task at hand, especially in an industrial environment where

the operations performed are often repetitive and physically demanding.

It is ultimately possible to account for these preferences through the adaptive compliance framework expressed in Sec. 3.4. Firstly, by activating the optimal ergonomics task (21) when human and robot are collaborating, we can ensure optimal human posture. From this, the operator preferences in the form of displacement from the actual pose are accommodated by switching to *human interaction* mode (Fig. 5) when the human interacts with the robot. A practical example is provided in the experiments in Sec. 4.3. This leads ultimately to a single framework, capable of balancing both between optimal human ergonomics and preference online, based on their relative priority.

3.6. Limitations and Advantages

The proposed scheme acts on the state augmentation, inherently increasing its computational load. With respect to a standard HQP-based controller in which the computational time is proportional to pn , with the AHQP scheme this increases as $(p+1)(n+m)$, given the m additional optimization variables at each solution of the QP problem, and the additional hierarchical level which must be considered for the regulation of \mathbf{x}_d . This additional level can be either occupied by the optimal ergonomics function, or by the Cartesian task in (26). As it will be seen in the experiments, it is possible to alternate between the two, depending on the application.

On the other hand, one of the main advantages involves the possibility of formulating both objective functions and constraints directly as functions of the Cartesian coordinate \mathbf{x}_d . With respect to a standard HQP, this avoids the addition of the pseudoinverse matrix \mathbf{J}^\dagger and thus of

$$\dot{\mathbf{q}}^T \mathbf{J}^\dagger \mathbf{J} \dot{\mathbf{q}} \quad (27)$$

when defining Cartesian space tasks such as (18). Similarly, when considering spatial constraints on \mathbf{x}_d as in (8), we can avoid to explicitly write the forward kinematics for both upper and lower bounds. This reduces computational times dissimilarities with respect to a standard HQP, when considering all the Cartesian constraints active for both controllers.

Regarding stability, it is proven in the literature [15] how the HQP formulation maintains a stable and continuous behavior even in the case in which the global optimum lies outside the bounds defined via the constraints. Indeed, in this case the system will reach the boundary and stop at the optimal limit, which does not imply an unstable behavior.

Another important aspect is the one related to the continuity of the shared workspace when abruptly changing its bounds (boundary boxes of Fig. 1, right). While it is necessary to ensure that the actual position of the EE lies within the new boundaries, a smooth transition of such boundaries from one time instant to the next is not required, as sudden variations of the boundaries will not affect control output continuity.

Lastly, the ergonomics map defined with our method is valid for subjects with similar kinematics, which on the one hand implies the definition of multiple mappings for very dissimilar

operators, but on the other hand provides a possibility of personalization, which is in line with the concept of the specific operator's preference proposed (Sec. 3.5).

4. Experiments and Results

The proposed framework was validated using the MOBILE Collaborative robotic Assistant (MOCA), a collaborative mobile manipulator composed by a Franka Emika Panda robotic arm and a Franka gripper, which is mounted on top of a Robotnik SUMMIT-XL STEEL mobile platform. The manipulator is torque controlled and the actuation torques are obtained from the lower level joint impedance controller in (5) (Fig. 5). The mobile platform is velocity controlled and the optimal velocities $\dot{\mathbf{x}}_{base}$ obtained are sent directly, based on the following decomposition of the state variable:

$$\mathbf{x} = \begin{bmatrix} \dot{\mathbf{q}} \\ \dot{\mathbf{x}}_d \end{bmatrix} = \begin{bmatrix} \dot{\mathbf{q}}_{base} \\ \dot{\mathbf{q}}_{arm} \end{bmatrix} = \begin{bmatrix} \dot{\mathbf{x}}_{base} \\ \dot{\mathbf{q}}_{arm} \end{bmatrix} \quad (28)$$

where $\dot{\mathbf{x}}_{base} = (\dot{x}, \dot{y}, \dot{\theta})$ is composed by the linear and angular velocities of the mobile base in the horizontal plane. In addition, using the MOCA platform, we further increase the degree of redundancy considered in our previous work, which allows to enlarge the stack of tasks ($m = 6$ and $n = 10$). The *threshold* on e_q is 0.2rad.

To properly show the feasibility and flexibility of the proposed control scheme, we considered various types of applications. In particular, three experiments were performed and will be reported in this section, after a brief explanation of the setup for the acquisition of the ergonomics scores.

4.1. Ergonomic Assessment Via Skeletal Tracking

For the mapping of the human ergonomics function defined in Sec. 3.1, we opted for a vision-based skeleton tracker algorithm, with the objective of avoiding the operator having to wear any cumbersome sensor that is often impractical and not suited in industrial environments. We used an RGB-D camera (Intel RealSense D435i) to track the skeletal key-points through an OpenPose [37] pre-trained deep learning method, from which we extract the joint positions \mathbf{q}_h .

We performed multiple offline acquisitions of the skeletal key-points, asking the subjects to reach with the dominant hand multiple target points (position only) in the workspace, without changing feet position. Each subject is also asked to reach the points in the most natural configuration and orientation possible. As mentioned in Sec. 3.1, this allows to restrict from infinite orientation and postural possibilities for each target point, to a smaller set dictated by the fact that the human will reach for a specific point always with similar orientations and postures, driven by the lowest muscular effort employed. From this set, we first consider the average orientation among all subjects as a reference value, and we then associate to each key-point of the hand (position + orientation) the ergonomics score calculated from the skeleton acquisitions (as in Sec. 3.1). These

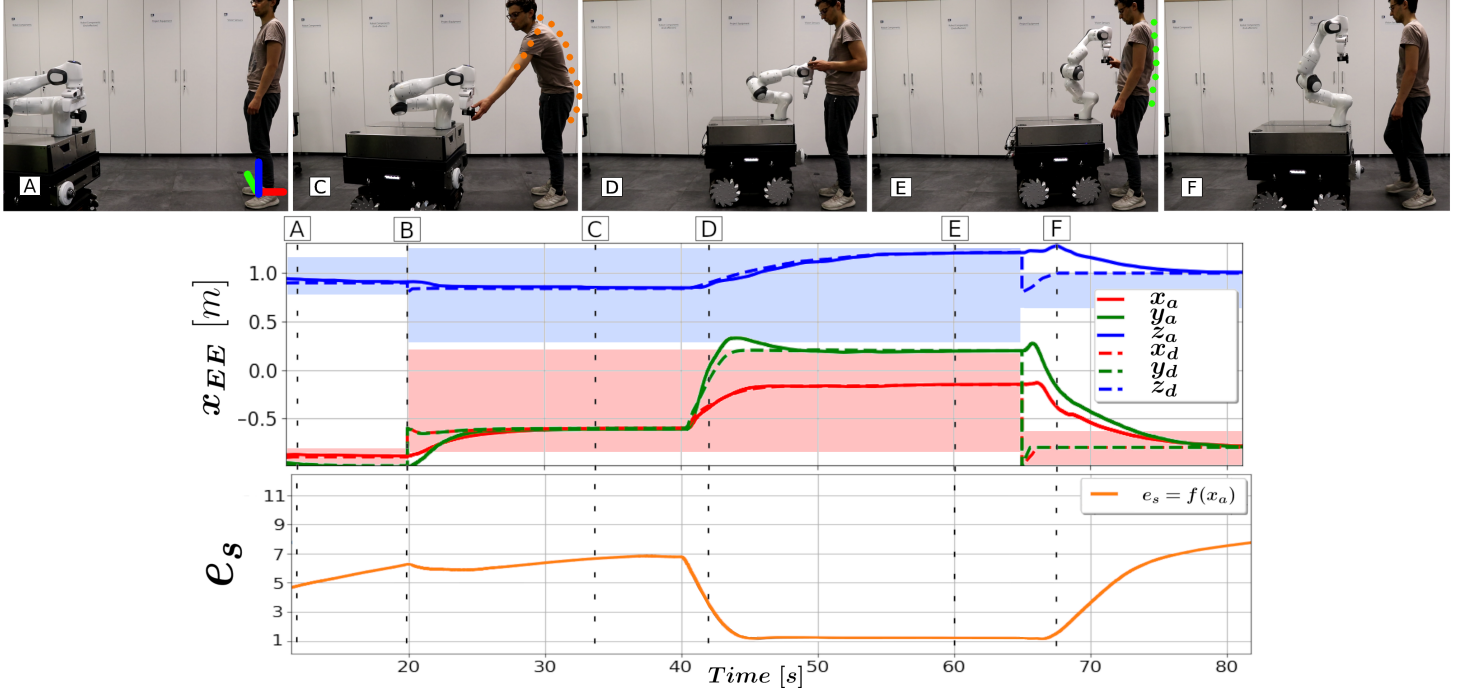


Figure 6: Experiment 1 snapshots taken during the task (top). Top plot of the bottom figures compares actual \mathbf{x}_a and desired \mathbf{x}_d EE trajectories. Their respective error is made to converge thanks to (6). The coloured regions indicate the feasible area for each component (same for x and y components, in red), based on the constraints on \mathbf{x}_d (as visible from Fig. 1). These are used to identify the shared workspace in which to find the optimal pose based on the objectives assigned. The bottom plot shows the ergonomics score as a function of \mathbf{x}_a .

key-points are then expressed in local human frame (feet position) allowing to calculate the ergonomics score regardless of the distance from the robot. We account for this distance in the online phase, in which it is sufficient to identify the position of the feet in world frame, in order to ultimately obtain \mathbf{H}_{ergo} and \mathbf{g}_{ergo} by interpolating in world frame (Fig. 4). These are used online to optimize \mathbf{x}_d in world frame.

Another advantage of this procedure is related to the use of the online camera exclusively for the acquisition of the position of the feet, avoiding data about the hands or other fast-moving joints that are often known to provide inaccurate and non-smooth measurements [38].

4.2. Experiment 1: Optimal Ergonomics Activation

The aim of the first experiment is to show the improvements relative to the activation of the maximum ergonomics objective function (21) during a collaborative task. The overall setup is shown in Fig. 6, where the robot delivers an object to a human operator, who subsequently works on the component by inserting screws. The item is then returned to the robot and sent to the following workstation. We choose this setup so that in the first part the robot approaches the human only following a policy of minimum distance from its initial position and thus minimum time, without activation of the minimum ergonomics score function (21). Only after handing the piece, optimal ergonomics is activated so that when the operator returns it to the robot, he/she will have to naturally assume a healthier and more ergonomic posture due to the new optimized handover position, thus increasing the quality of the task both quantitatively

(in terms of ergonomics score) and qualitatively (in terms of accumulated physical and mental fatigue, as reported by the subjects). Overall, the task's time is not increased since the robot reconfigures during a passive phase (while the human is working on the object).

The top plot of Fig. 6 compares the actual \mathbf{x}_a and the desired \mathbf{x}_d EE trajectories, showing the feasibility region along each direction with the respective colour (same for x and y directions in red), corresponding to the bounds defined on \mathbf{x}_d in the constraints definition phase of Algorithm 1. The robot is originally in steady conditions (A). Based on the actual human position, the new set of constraints is updated (B) so that the human position lies in the middle of the (coloured) feasible area. This avoids having to define a specific pose for the handover at planning level (also avoiding complex planning algorithms [40, 41]), rather defining a shared area in which the physical interaction can take place, and in which the final handover pose will be optimized according to the priorities in the hierarchy.

We consider step variations of the boundary regions (defined at constraint level) as they do not affect continuity (as stated in 3.6), which is still ensured by the constraints on $\dot{\mathbf{x}}_d$, $\ddot{\mathbf{x}}_d$. Indeed, by imposing more restrictive constraints on $\ddot{\mathbf{x}}_d$ it is possible to achieve a longer and smoother transitioning region, based on the specific task (transitioning interval spans from time $t = 20$ s to $t = 25$ s).

Having to reach the operator as fast as possible, in (B) the priority is given to the minimum path in order to quickly hand-over the object. As visible from the corresponding picture in (C), the robot stops upon reaching the shared workspace,

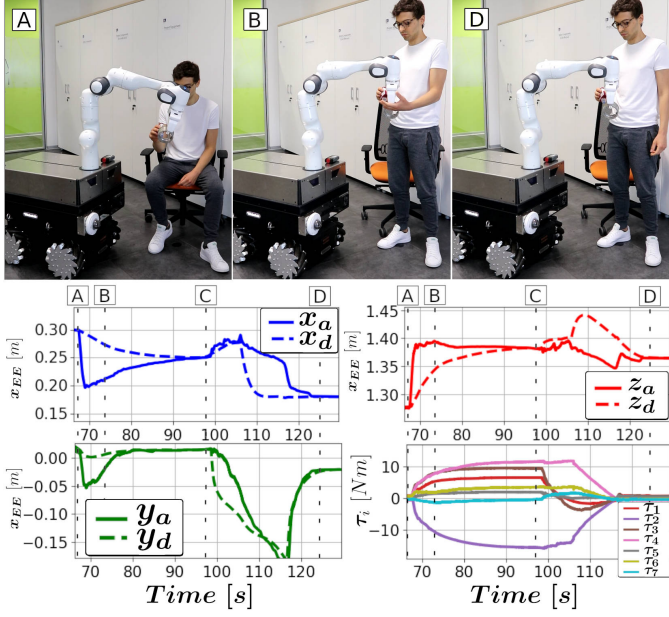


Figure 7: Experiment 2 key snapshots of the task (top). After standing up, the human moves the EE to comfortably continue working on the piece held by the EE. The plots compare each component of the actual vs desired EE position (x -axis top left, y -axis bottom left, z -axis top right) and arm actuation torques τ_i (bottom right).

forcing the operator to assume a very poor posture. This is quantified in the bottom plot, in which the ergonomics score e_s indicates a high risk, suggesting a quick change in position. At $t = 40s$, while the human works on the object, the ergonomics function is activated and the robot starts to reconfigure (D) eventually reaching the best ergonomics point dictated by the mapping (Fig. 4) as far as possible, based on the other priorities. The parameters H_{ergo} and g_{ergo} are obtained online thanks to the offline acquisitions in human coordinate frame (Sec. 4.1) and the online human position in world frame, and are then passed to the AHQP. Here we denote a considerable decrease in the ergonomics score, passing from $e_s = 7$ (C) to $e_s = 1$ (E), indicating a remarkable ergonomics improvement and leading to almost no risk for the second handover pose. It must be noted that the base of the robot comes closer to the human in (E), given that the optimal point obtained from the ergonomics map offline is high in the reachable workspace of the robot, and would be unreachable otherwise. Finally, the robot grabs the piece and both the constraints and the hierarchy are updated to reach the new goal (F). In particular, optimal ergonomics task is swapped with the Cartesian reference task (26), so that the robot can precisely reach the following target pose to place the object. The experiment was repeated on five healthy subjects, showing always similar ergonomics score improvements upon task activation, important with repeated and prolonged physical efforts, to reduce MSDs. The calculation time alternates from a maximum of 1ms when in *human interaction* mode, to 2ms when in *human ergonomics* mode.

These results can be potentially exploited for any collaborative scenario, in which the robot is required to optimize human

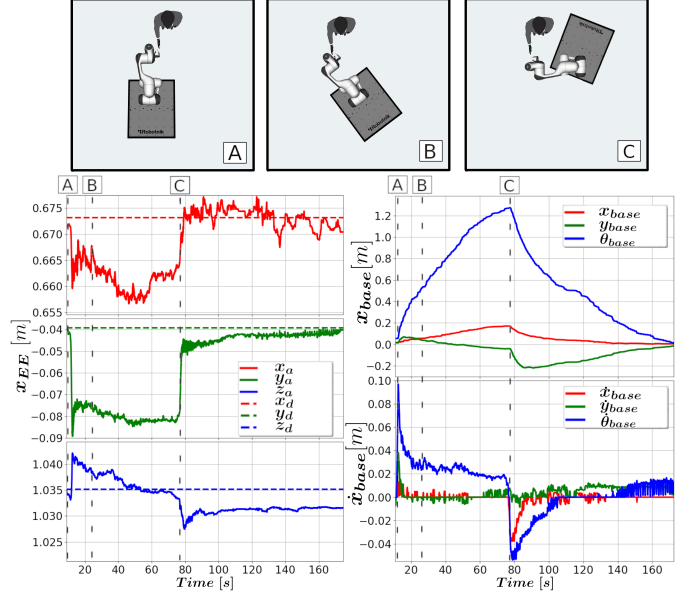


Figure 8: Experiment 2. Comparison with respect to a standard whole-body impedance controller [39] for a mobile manipulator equipped with a velocity controlled mobile base. From the equilibrium, the human pulls the EE (B) generating an opposing force, until the EE is released (C). Top figures depict the behaviour of the base.

ergonomics among any other task.

4.3. Experiment 2: Human Preference

Our second experiment uses the adaptive compliance scheme of Sec. 3.4, showing the complete ergonomics-aware AHQP framework, capable of optimizing both human ergonomics and preference. Here the operator applies some glue on the workpiece held by the robot (Fig. 7). Indeed, while the operator is initially sitting, he might decide to stand up (or vice versa) to change or alternate his/her position based on preference. Indeed, since the position of the feet is not altered, the ergonomics objective function would not be capable of optimizing x_{EE} for better posture, thus not considering the human change. For these cases, it is useful to perform adjustments on the EE directly by the user. Indeed, to make the task more comfortable, now the human can move the robot to a better pose (still inside of the feasibility regions defined, similarly to Fig. 6 for Experiment 1), while continuing with the gluing task. In the case of a standard impedance controller, the forces exerted from the robot would be proportional to the imparted displacement, and they would keep constant in time, thus tiring the operator quickly. We provide instead a degree of flexibility through the force adaptation of the adaptive framework.

More in detail, after the EE is moved by the person (Fig. 7-B), the joint error will increase (as explained in Sec. 3.4) and the stack of tasks changes from *human ergonomics* to *human interaction* (Fig. 5), removing the tasks involving x_d . Thereby, the person feels a first counteracting force in (B), visible from the actuation torques τ_i (Fig. 7, bottom right), which is the same he would have felt with a standard impedance controller. However, thanks to the variation in (6) of x_d (Fig. 7, x_{EE} plots),

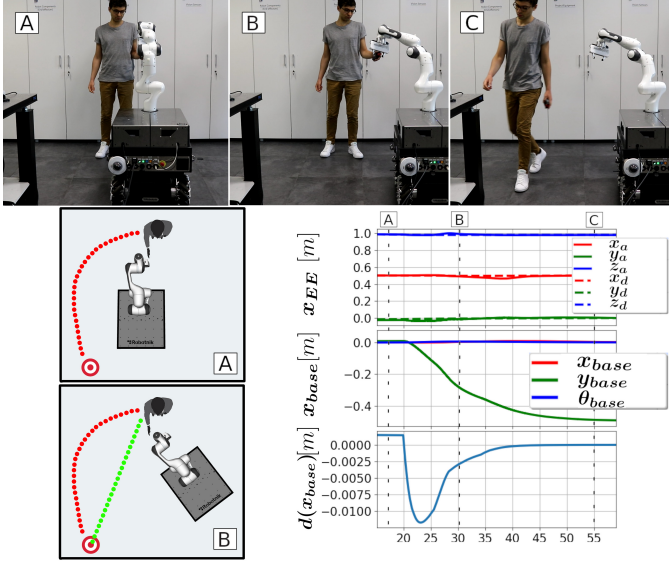


Figure 9: Experiment 3 snapshots (top). Bottom right plots show EE \mathbf{x}_{EE} (top) and base \mathbf{x}_{base} (middle) trajectories, with distance objective function $d(\mathbf{x}_{base})$ (bottom). Bottom left figures show a top view of the human trajectory improvements achieved.

the opposing torques will start diminishing in (C). They keep reducing, and eventually the new EE position becomes the equilibrium one (D), allowing the operator to continue working with improved posture and better ergonomics with respect to the previous condition. Overall, the variation of the desired Cartesian reference (dashed lines) allowed to move the EE of approximately 0.16m in task space.

The same experiment is conducted using a standard whole-body impedance controller for a mobile manipulator as in [39]. Clearly, the adaptive behaviour of the proposed controller is not achievable in this case, as the reference trajectories are provided from planning stage. We can further notice that when the person starts pushing the EE as in Fig. 8 (A) the mobile base will exert an opposite force by starting its rotation, as shown in the top right plot of Fig. 8 (\mathbf{x}_{base}). For prolonged physical interaction though, and until the forcing action is released by the person (C), the base will keep rotating as shown. This is due to the admittance formulation of the velocity-controlled mobile base, for which a constant velocity is generated through the admittance model, when the virtual torques remain constant (Fig. 8, bottom right). As a result, for prolonged interactions the base orientation will diverge substantially from the original one, creating problems both in terms of task accomplishment and of safety, by potentially impacting with the human.

4.4. Experiment 3: Human Intentions

This final experiment allows to facilitate human's future intentions by formulating particular tasks in the same hierarchy and ergonomics-aware AHQP control framework, to improve the overall performance metrics. Being out of our scope, we are not dealing with the possible ways of recognizing human's future intention (e.g. line of sight detection, physical gestures or behaviours), instead we simply consider the intention as the

path leading to the next workstation. We can then formulate in the stack of tasks an objective that will maximize the mobile base distance from such target $\mathbf{x}_t \in \mathbb{R}^3$ as:

$$\max_{\chi} d(\mathbf{x}_{base}) = \min_{\chi} -\|\mathbf{x}_{base} - \mathbf{x}_t\|^2 = \min_{\chi} -\left\| \begin{bmatrix} \Delta t \mathbf{I}_{3 \times n} & \mathbf{0}_{3 \times m} \end{bmatrix} \begin{bmatrix} \dot{\mathbf{q}} \\ \dot{\mathbf{x}}_d \end{bmatrix} - (\mathbf{x}_t - \mathbf{x}_{base_{t-1}}) \right\|^2. \quad (29)$$

The setup is shown in Fig. 9, in which after the collaborative phase (A), the human intention is to reach the table on his right. To ensure that the mobile base is not in the way, (29) is activated in the hierarchy (B) ultimately allowing the operator to easily reach the table (C) without obstacles and in shorter time. The top plot shows how the actual EE trajectory \mathbf{x}_a keeps tracking the desired \mathbf{x}_d while the base \mathbf{x}_{base} rearranges (middle plot). The bottom plot depicts the increase (absolute value) of the distance function $d(\mathbf{x}_{base})$. It must be noted that in this last experiment all three aspects of human ergonomics, preference and intention are active together, allowing their balanced relative prioritization based on the task hierarchy. This results in the optimal trade-off between human- and performance-based indexes.

5. Discussion and Conclusions

We have introduced the optimization of human ergonomics in a hierarchical controller, by exploiting the AHQP scheme and formulating an objective function based on the ergonomics score. The resulting Ergonomics-Aware AHQP brings several advantages in collaborative tasks in terms of adaptation to human ergonomics (and comfort), preferences, and intentions. Experiment 1 assessed human postural improvements, proving the potential benefits under long-term repetitive loading cycles, often linked to MSDs. Experiment 2 included human preference in the same framework, while still optimizing ergonomics. Indeed, a trade-off between the two is not considered in existing methods or it is often strongly task-dependent. We provide a flexible framework to accommodate for both, by adapting the robot compliance based on the type of interaction, thus accommodating human interactions while rejecting external disturbances. In the last experiment we facilitate human intentions and further reduce cycle times.

Overall, our key contribution is to provide a unique framework, highlighting the human figure in common industrial operations, without compromising productivity. A limitation however involves the autonomous regulation of the hierarchy based on the task at hand for better integration in real scenarios. Future developments will address these issues, together with the addition of robot dynamics for multiple robots/humans collaboration.

Declaration of competing interest

The authors declare that they have no known competing financial interests or personal relationships that could have appeared to influence the work reported in this paper.

Acknowledgment

This work was supported in part by the ERC-StG Ergo-Lean (Grant Agreement No. 850932), in part by the European Union's Horizon 2020 research and innovation programme under Grant Agreement No. 871237 (SOPHIA).

References

- [1] A. Liegeois, Automatic supervisory control of the configuration and behavior of multibody mechanisms, *IEEE Trans. Systems, Man, and Cybernetics* 7 (12) (1977) 842–868.
- [2] H. Hanafusa, T. Yoshikawa, Y. Nakamura, Analysis and control of articulated robot arms with redundancy, *IFAC Proceedings Volumes* 14 (2) (1981) 1927–1932. doi:[https://doi.org/10.1016/S1474-6670\(17\)63754-6](https://doi.org/10.1016/S1474-6670(17)63754-6).
- [3] J. Hollerbach, K. Suh, Redundancy resolution of manipulators through torque optimization, *IEEE Journal on Robotics and Automation* 3 (4) (1987) 308–316.
- [4] P. Hsu, J. Mauser, S. S. Sastry, Dynamic control of redundant manipulators, *J. Field Robotics* 6 (1989) 133–148.
- [5] B. Siciliano, J.-J. Slotine, A general framework for managing multiple tasks in highly redundant robotic systems, in: 5th International Conference on Advanced Robotics, IEEE, 1991, pp. 1211–1216.
- [6] O. Khatib, A unified approach for motion and force control of robot manipulators: The operational space formulation, *IEEE Journal on Robotics and Automation* 3 (1) (1987) 43–53.
- [7] O. Khatib, K. Yokoi, K. Chang, D. Ruspini, R. Holmberg, A. Casal, Vehicle/arm coordination and multiple mobile manipulator decentralized co-operation, in: Proceedings of IEEE/RSJ International Conference on Intelligent Robots and Systems. IROS '96, Vol. 2, 1996, pp. 546–553 vol.2. doi:[10.1109/IROS.1996.570849](https://doi.org/10.1109/IROS.1996.570849).
- [8] K. Bouyarmane, K. Chappellet, J. Vaillant, A. Kheddar, Quadratic programming for multirobot and task-space force control, *IEEE Transactions on Robotics* 35 (1) (2019) 64–77. doi:[10.1109/TRO.2018.2876782](https://doi.org/10.1109/TRO.2018.2876782).
- [9] T. Li, O. Kermorgant, A. Krupa, Maintaining visibility constraints during tele-echography with ultrasound visual servoing, *IEEE International Conference on Robotics and Automation* (2012) 856–861 doi:[10.1109/ICRA.2012.6224974](https://doi.org/10.1109/ICRA.2012.6224974).
- [10] F. Tassi, S. Gholami, E. De Momi, A. Ajoudani, A reconfigurable interface for ergonomic and dynamic tele-locomanipulation, in: 2021 IEEE International Conference on Intelligent Robots and Systems (IROS), IEEE, 2021 [ACCEPTED].
- [11] J. Park, O. Khatib, Contact consistent control framework for humanoid robots, in: Proceedings IEEE International Conference on Robotics and Automation ICRA 2006., IEEE, 2006, pp. 1963–1969.
- [12] O. Khatib, L. Sentis, J.-H. Park, A unified framework for whole-body humanoid robot control with multiple constraints and contacts, in: European Robotics Symposium 2008, Springer, 2008, pp. 303–312.
- [13] J. Salini, V. Padois, P. Bidaud, Synthesis of complex humanoid whole-body behavior: A focus on sequencing and tasks transitions, in: 2011 IEEE International Conference on Robotics and Automation, IEEE, 2011, pp. 1283–1290.
- [14] Y. Abe, M. Da Silva, J. Popović, Multiobjective control with frictional contacts, in: 2007 ACM SIGGRAPH/Eurographics symposium on Computer animation, 2007, pp. 249–258.
- [15] A. Escande, N. Mansard, P.-B. Wieber, Hierarchical quadratic programming: Fast online humanoid-robot motion generation, *The International Journal of Robotics Research* 33 (7) (2014) 1006–1028.
- [16] L. Saab, O. E. Ramos, F. Keith, N. Mansard, P. Soueres, J.-Y. Fourquet, Dynamic whole-body motion generation under rigid contacts and other unilateral constraints, *IEEE Transactions on Robotics* 29 (2) (2013) 346–362.
- [17] O. Kanoun, F. Lamiroux, P.-B. Wieber, Kinematic control of redundant manipulators: Generalizing the task-priority framework to inequality task, *IEEE Transactions on Robotics* 27 (4) (2011) 785–792.
- [18] N. Mansard, O. Khatib, A. Kheddar, A unified approach to integrate unilateral constraints in the stack of tasks, *IEEE Transactions on Robotics* 25 (3) (2009) 670–685. doi:[10.1109/TRO.2009.2020345](https://doi.org/10.1109/TRO.2009.2020345).
- [19] F. Tassi, E. De Momi, A. Ajoudani, Augmented hierarchical quadratic programming for adaptive compliance robot control, in: 2021 IEEE International Conference on Robotics and Automation (ICRA), IEEE, 2021, pp. 3568–3574.
- [20] G. Brantner, O. Khatib, Controlling ocean one: Human–robot collaboration for deep-sea manipulation, *Journal of Field Robotics* 38 (1) (2021) 28–51. doi:<https://doi.org/10.1002/rob.21960>.
- [21] W. Kim, M. Lorenzini, P. Balatti, P. Nguyen, U. Pattacini, V. Tikhonoff, L. Peternel, C. Fantacci, et al., A reconfigurable and adaptive human-robot collaboration framework for improving worker ergonomics and productivity, *IEEE Robotics and Automation Magazine* (2019).
- [22] P. Tsarouchi, S. Makris, G. Chryssolouris, Human–robot interaction review and challenges on task planning and programming, *International Journal of Computer Integrated Manufacturing* 29 (8) (2016) 916–931. doi:[10.1080/0951192X.2015.1130251](https://doi.org/10.1080/0951192X.2015.1130251).
- [23] K. Otani, K. Bouyarmane, S. Ivaldi, Generating assistive humanoid motions for co-manipulation tasks with a multi-robot quadratic program controller, in: 2018 IEEE International Conference on Robotics and Automation (ICRA), 2018, pp. 3107–3113. doi:[10.1109/ICRA.2018.8463167](https://doi.org/10.1109/ICRA.2018.8463167).
- [24] A. Rocchi, E. M. Hoffman, D. G. Caldwell, N. G. Tsagarakis, Opensot: a whole-body control library for the compliant humanoid robot coman, in: 2015 IEEE International Conference on Robotics and Automation (ICRA), IEEE, 2015, pp. 6248–6253.
- [25] L. Peternel, C. Fang, N. Tsagarakis, A. Ajoudani, A selective muscle fatigue management approach to ergonomic human-robot co-manipulation, *Robotics and Computer-Integrated Manufacturing* 58 (2019) 69–79. doi:<https://doi.org/10.1016/j.rcim.2019.01.013>.
- [26] S. Hignett, L. McAtamney, Rapid entire body assessment (reba), *Applied Ergonomics* 31 (2) (2000) 201–205. doi:[https://doi.org/10.1016/S0003-6870\(99\)00039-3](https://doi.org/10.1016/S0003-6870(99)00039-3).
- [27] W. Kim, L. Peternel, M. Lorenzini, J. Babič, A. Ajoudani, A human-robot collaboration framework for improving ergonomics during dexterous operation of power tools, *Robotics and Computer-Integrated Manufacturing* 68 (2021) 102084. doi:<https://doi.org/10.1016/j.rcim.2020.102084>.
- [28] M. Middlesworth, A step-by-step guide to the reba assessment tool, (last accessed: 11.12.2021). URL <https://ergo-plus.com/reba-assessment-tool-guide>
- [29] A. Dietrich, C. Ott, J. Park, The hierarchical operational space formulation: Stability analysis for the regulation case, *IEEE Robotics and Automation Letters* 3 (2) (2018) 1120–1127. doi:[10.1109/LRA.2018.2792154](https://doi.org/10.1109/LRA.2018.2792154).
- [30] A. Dietrich, C. Ott, Hierarchical impedance-based tracking control of kinematically redundant robots, *IEEE Transactions on Robotics* 36 (1) (2020) 204–221. doi:[10.1109/TRO.2019.2945876](https://doi.org/10.1109/TRO.2019.2945876).
- [31] Y. Wang, L. Wang, Whole-body collision avoidance control design using quadratic programming with strict and soft task priorities, *Robotics and Computer-Integrated Manufacturing* 62 (2020) 101882. doi:<https://doi.org/10.1016/j.rcim.2019.101882>.
- [32] C. Ott, R. Mukherjee, Y. Nakamura, A hybrid system framework for unified impedance and admittance control, *Journal of Intelligent & Robotic Systems* 78 (06 2014). doi:[10.1007/s10846-014-0082-1](https://doi.org/10.1007/s10846-014-0082-1).
- [33] F. Keith, P.-B. Wieber, N. Mansard, A. Kheddar, Analysis of the discontinuities in prioritized tasks-space control under discrete task scheduling operations, in: 2011 IEEE/RSJ International Conference on Intelligent Robots and Systems, 2011, pp. 3887–3892. doi:[10.1109/IROS.2011.6094706](https://doi.org/10.1109/IROS.2011.6094706).
- [34] J. Lee, N. Mansard, J. Park, Intermediate desired value approach for task transition of robots in kinematic control, *IEEE Transactions on Robotics* 28 (6) (2012) 1260–1277. doi:[10.1109/TRO.2012.2210293](https://doi.org/10.1109/TRO.2012.2210293).
- [35] G. Jarquín, A. Escande, G. Arechavaleta, T. Moulard, E. Yoshida, V. Parra-Vega, Real-time smooth task transitions for hierarchical inverse kinematics, in: 2013 13th IEEE-RAS International Conference on Humanoid Robots (Humanoids), 2013, pp. 528–533. doi:[10.1109/HUMANOIDS.2013.7030024](https://doi.org/10.1109/HUMANOIDS.2013.7030024).
- [36] S. Kim, K. Jang, S. Park, Y. Lee, S. Y. Lee, J. Park, Continuous task transition approach for robot controller based on hierarchical quadratic programming, *IEEE Robotics and Automation Letters* 4 (2) (2019) 1603–1610.
- [37] Z. Cao, G. Hidalgo, T. Simon, S.-E. Wei, Y. Sheikh, Openpose: realtime multi-person 2d pose estimation using part affinity fields, *IEEE transactions on pattern analysis and machine intelligence* 43 (1) (2019) 172–186.

- [38] Y. Liu, J. Chen, C. Hu, Y. Ma, D. Ge, S. Miao, Y. Xue, L. Li, Vision-based method for automatic quantification of parkinsonian bradykinesia, *IEEE Transactions on Neural Systems and Rehabilitation Engineering* 27 (10) (2019) 1952–1961. doi:10.1109/TNSRE.2019.2939596.
- [39] A. Dietrich, T. Wimböck, A. Albu-Schäffer, Dynamic whole-body mobile manipulation with a torque controlled humanoid robot via impedance control laws, in: 2011 IEEE/RSJ International Conference on Intelligent Robots and Systems, 2011, pp. 3199–3206. doi:10.1109/IROS.2011.6094445.
- [40] L. Lu, J. Zhang, J. Y. H. Fuh, J. Han, H. Wang, Time-optimal tool motion planning with tool-tip kinematic constraints for robotic machining of sculptured surfaces, *Robotics and Computer-Integrated Manufacturing* 65 (2020) 101969. doi:https://doi.org/10.1016/j.rcim.2020.101969.
- [41] V. Montreuil, A. Clodic, M. Ransan, R. Alami, Planning human centered robot activities, in: 2007 IEEE International Conference on Systems, Man and Cybernetics, 2007, pp. 2618–2623. doi:10.1109/ICSMC.2007.4413992.